ISSN 0020-4412, Instruments and Experimental Techniques, 2007, Vol. 50, No. 2, pp. 187–195. © Pleiades Publishing, Ltd., 2007.
Original Russian Text © A.G. Voronin, V.M. Grebenyuk, D.E. Karmanov, N.A. Korotkova, Z.V. Krumshtein, M.M. Merkin, A.Yu. Pakhomov, D.M. Podorozhnyi, A.B. Sadovskii, L.G. Sveshnikova, L.G. Tkachev, A.N. Turundaevskii, 2007, published in Pribory i Tekhnika Eksperimenta, 2007, No. 2, pp. 50–58.

NUCLEAR EXPERIMENTAL TECHNIQUE

Testing a Prototype of the Charge-Measuring System for the NUCLEON Setup

A. G. Voronin[a], V. M. Grebenyuk[b], D. E. Karmanov[a], N. A. Korotkova[a], Z. V. Krumshtein[b], M. M. Merkin[a], A. Yu. Pakhomov[a], D. M. Podorozhnyi[a], A. B. Sadovskii[b], L. G. Sveshnikova[a], L. G. Tkachev[b], and A. N. Turundaevskii[a]

[a] *Skobel'tsyn Institute of Nuclear Physics, Moscow State University, Vorob'evy gory 1, str. 2, Moscow, 119992 Russia*
[b] *Joint Institute for Nuclear Research, ul. Joliot-Curie 6, Dubna, Moscow oblast, 141980 Russia*

Received May 29, 2006; in final form, July 11, 2006

Abstract—While preparing for the NUCLEON experiment, a prototype of the experimental setup was tested on a beam of high-energy ions. The response of the charge-measuring system was investigated. The test experiment was simulated. The simulated charge distributions were compared to the experimental data.

PACS numbers: 29.30.Ep, 29.40.Gx, 96.50.sb

DOI: 10.1134/S0020441207020030

INTRODUCTION

One of the most important astrophysical problems is to study the origin and propagation of primary cosmic rays (CRs) in the Galaxy. An essential deficiency of cosmic-ray physics is the absence of comprehensive data on the charge composition of CRs in the range of >10 TeV. A study of the charge and isotope composition of low-energy CRs has made it possible to determine (basically, by analyzing the ratio of the secondary nuclei, derived from fragmentation by interstellar medium nuclei, to the primary nuclei—B/C, V/Fe, etc.) that, according to the present-day models, CR propagation of cosmic rays is of diffusion nature and their lifetime before escape from the Galaxy is very long (~7×10^7 yr and more). Therefore, prior to reaching the Earth, CRs with an energy of ~1 GeV pass through a thick layer of material (~10 g/cm^2). For higher-energy particles, the thickness of the material decreases sharply (at an energy of 10 TeV, it is 0.1–0.4 g/cm^2), which is expected to cause the spectra observed near the Earth's surface to differ from the spectra of CR sources.

The experimental testing of the models consisted only in verifying the relationship between the secondary and primary nuclei. Therefore, investigation of the charge composition of CRs with discrimination between elements in the high-energy region is a key to solving the problems of origin and propagation of CRs in the Galaxy [1].

The energy spectrum of primary CRs shows a steep decline; therefore, to obtain essential statistics at high energies, it is required that an experimental setup have a large geometrical factor. However, placing an instrument aboard a spacecraft entails rigid mass limitations. A new method has recently been proposed for measuring the spectra of primary CR particles by recording (using microstrip silicon arrays) the spatial density of secondary charged particles produced by interactions of primary particles inside the setup [2]. It was proposed that the charge of primary particles be simultaneously measured using silicon detectors that had already been employed to good effect to study CRs, e.g., in the ATIC experiment [3]. These detectors are divided into separate elements—the so-called pads. It is expected that this method for measuring the CR energy will be applied to the future NUCLEON experiment on board a satellite, and the use of several arrays of strip detectors will guarantee reliable determination of particle charges [4].

Simulation of the experiment was performed with the aids of the GEANT 3.21 software package [5] complemented by the QGSJET nuclear interaction generator [6, 7], which provides a means for describing high-energy hadron–nucleus and nucleus–nucleus interactions. In [8, 9], it was shown that the both methods for determining the energy and the charge were adequate to this task.

At the same time, it is necessary that preparations for the actual experiment involve experimental testing of the setup. The simplified prototype of the instrument was initially tested on the extracted H8 beam of the SPS accelerator at CERN (pions with an energy of 180 GeV) [10]. Results of the first test showed that the proposed technique allowed the energy of 180-GeV pions to be measured to be measured with a relative error of ~67%, which is in good agreement with the results of simulation (65%). The objective of the subsequent tests was to test equipment the structure of which is close to the actual one. In this case, both the energy

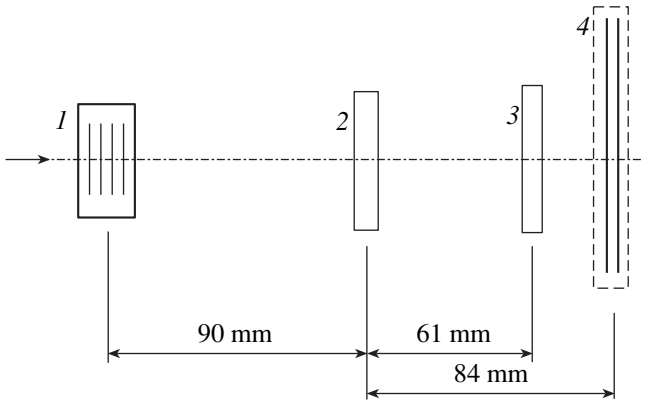

Fig. 1. Layout of the experiment on the ion beam in 2003: (*1*) charge-measuring system, (*2*) graphite target, (*3*) tungsten converter, and (*4*) microstrip detectors.

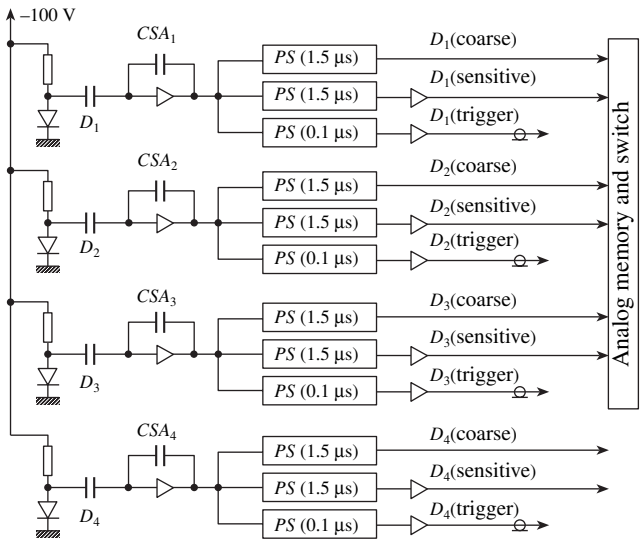

Fig. 2. Block diagram of the charge-measuring system: (*CSA*) charge-sensitive amplifier, (*PS*) pulse shaper, and (*D*) channels for detector data.

reconstruction technique and the charge-measuring system were tested.

In this paper, we describe in detail the procedure for testing the charge-measuring system on a beam of particles with different charges in the experiment at CERN.

DESCRIPTION OF THE EXPERIMENT

In the course of the experiment, a beam of indium nuclei with an energy of ~158 GeV/nucleon was directed toward a 4-cm-thick beryllium target. The secondary charged particles and nuclear fragments were then separated according to their rigidity by means of a magnetic deflection system. In the experiment, particles with rigidities of 157.65, 315.5, 319.0, and 339.56 GeV/Z (Z is the nuclear charge) were selected. Since the energy per nucleon was constant for all nuclei produced by fragmentation of indium, each value of the magnetic rigidity corresponded to a particular value of ratio of the mass number to the charge A/Z (1.000, 2.000, 2.023, and 2.154). It is evident that the first value corresponds only to protons; the second, to deuterium, α particles, ^{6}Li, ^{10}B, ^{12}C, etc.; the third, to ^{87}Tc or ^{89}Ru (instable isotopes with a very short lifetime); and the fourth, to ^{28}Al and ^{56}Fe.

Note that the distance between the beryllium target and the prototype of the NUCLEON setup was ~620 m. As a result, short-lived nuclei with lifetimes less than ~2 μs decayed without hitting the detector system.

The schematic diagram of the NUCLEON setup prototype used in the experiment on an accelerated beam of heavy nuclei is shown in Fig. 1. The following equipment was installed downstream of the beam:

(1) four layers of silicon detectors *1* for measuring the charge and generating a trigger;

(2) 10-mm-thick graphite target *2* in which incident nuclei (fragments) interacted with carbon nuclei;

(3) 10.5-mm-thick tungsten converter *3*, in which photons were converted into charged electron–positron pairs; and

(4) two arrays of silicon microstrip detectors *4* for measuring the number and relative positions of secondary particles produced after interaction of the primary particle.

Both groups of silicon detectors, along with the readout electronic system, were enclosed in metal cases that protected the detectors against light and electromagnetic interference. To reduce the amount of substance in the path of primary particles and thereby lower the probability of these particles interacting before hitting the target, holes were drilled in a thick wall of the case opposite the detectors and then covered by a thin metal foil.

All of the four units of the setup were installed on a thick steel platform so that their horizontal axes were located at equal heights above the platform. Nevertheless, each unit could move in a horizontal plane parallel to the platform surface and be fixed at any position.

The system for determining the charge consists of four arrays of silicon detectors composed of separate pads. Information on the incident particle charge is collected from each array independently of the others, which guarantees a higher accuracy of measurements than is achieved by a single array.

The detectors of the charge-measuring system are housed in a common metal lightproof case having a thin window in the path of the beam, so that the separation between the arrays is 5 mm. A system of fasteners connects the case with the detectors to the bearing surface of the metal base on which a board with a reader is installed. The base with the reader and the detector unit is fixed on the bed in a movable mount of the dovetail

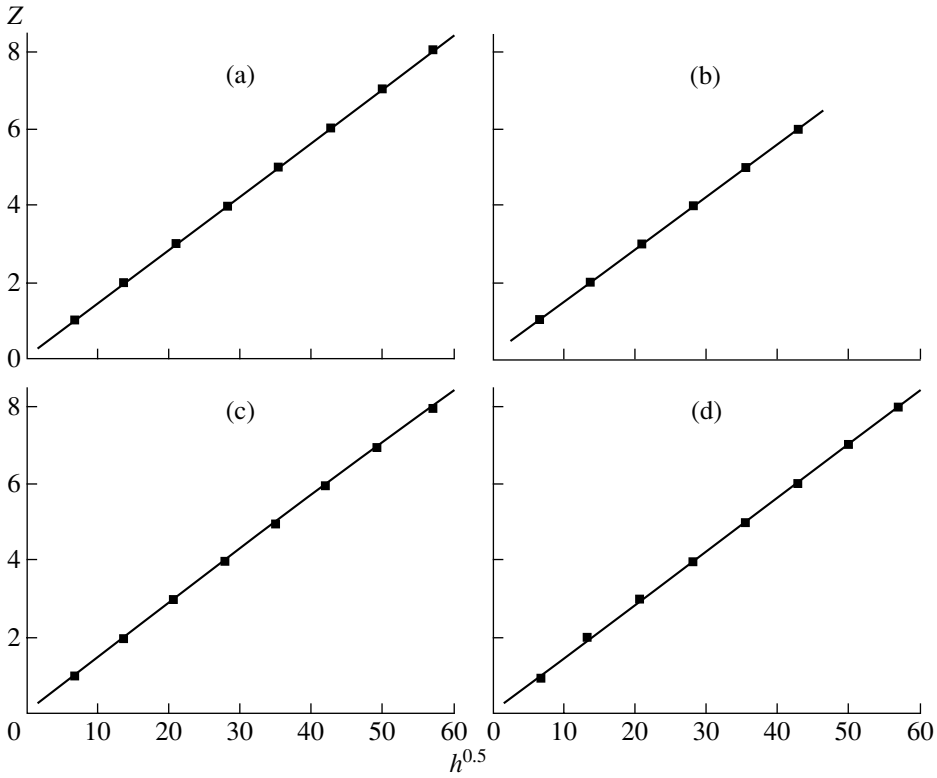

Fig. 3. Calibration curves for the sensitive channel: (a) the first, (b) second, (c) third, and (d) fourth layers.

type, which allows the unit to move in a horizontal direction in a plane perpendicular to the beam axis.

The first and second (downstream of the beam) detectors have dimensions of 1×1 cm, and the next two detectors measure 3×3 cm overall.

Apart from measuring the charge, the smaller (1×1 cm) detectors are used to bound the region of incidence of the primary particles in the case of a narrow beam and thereby limit the interaction zone inside the target. As a result, the interaction zone was located opposite the centers of the microstrip detectors and secondary particles escaping from it were detected with a maximum efficiency.

Each of the four ~0.4-mm-thick detectors was attached to a ceramic substrate ~0.8 mm thick. Therefore, the total material budget in the charge-measuring system was ~0.05 the radiation length.

The same ceramic substrate also carried a hybrid charge-sensitive amplifier with a significantly reduced noise level and a signal-to-noise ratio of ~20.

Three data acquisition channels followed each of the four preamplifiers (Fig. 2). The low-gain channel included a pulse shaper with a shaping time of ~1.5 μs, the high-gain channel consisted of a pulse shaper with a shaping time of 1.5 μs and a supplementary amplifier with a gain of ~20, and the triggering channel comprised a fast pulse shaper (0.1 μs) and a supplementary amplifier.

The signals from the low- and high-gain channels arrived at analog memory cells and then came to the analog switch that alternately connected them to the analog-to-digital converter (ADC). The availability of both sensitive and coarse data-acquisition channels for each detector has made it possible, using a 12-bit ADC, to cover the dynamic range of 0.1–1000 minimum ionizing particles (MIPs). (*MIP* denotes the most probable signal amplitude for such particles.)

The signals from the fast pulse shapers were transmitted over cables to four discriminator–shapers (with a shaping time of ~0.2 μs) and arrived at the circuit of triple or fourfold coincidences. The output signal of the coincidence circuit acted as a trigger, i.e., issued a command to record this coincidence. Three of the four discriminators had very low thresholds (~0.1*MIP*), which provided a means for recording absolutely all particles and, at the same time, for excluding random (other than produced by particles) operations of the instrument owing to the use of triple coincidences. The fourth discriminator had a high threshold (~4*MIP*) and was used to eliminate events due to single- and double-charged particles, which constituted the main flow of events. Only nuclei with $Z \geq 3$ were detected. This allowed us to record only those files in which the percentage of heavy nuclei was rather high and thereby to save hard disk space. The required number of particles with low charges (Z = 1–2) was collected very quickly when measuring triple coincidences.

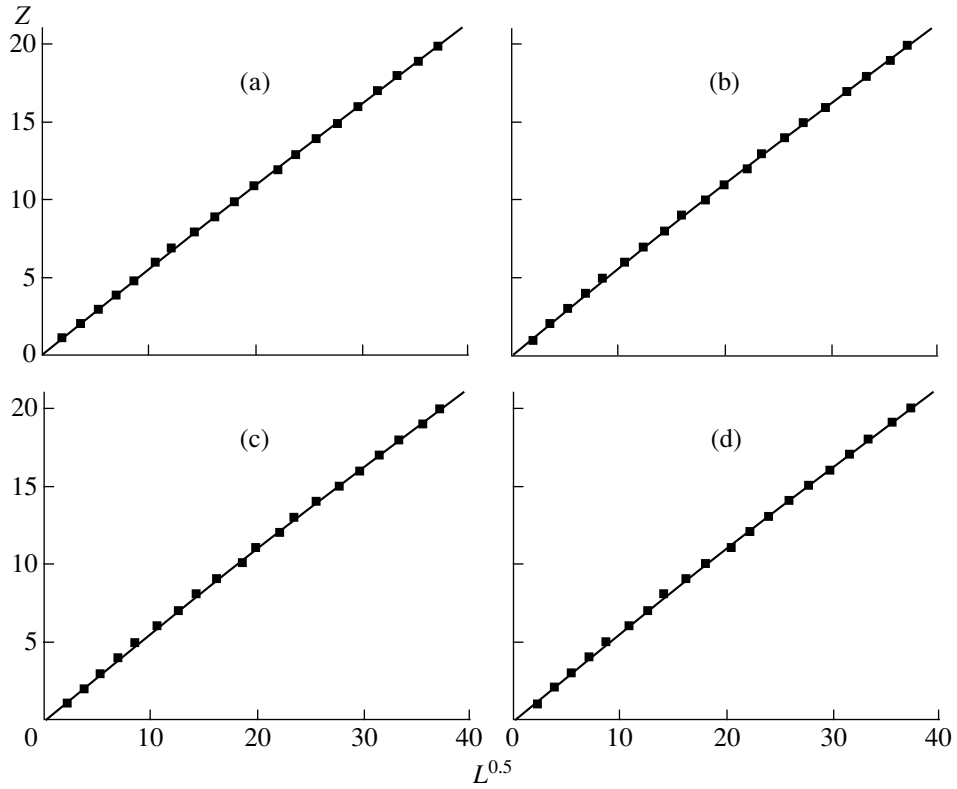

Fig. 4. Calibration curves for the coarse channel: (a) the first, (b) second, (c) third, and (d) fourth layers.

As noted above, the compactness of the first two detectors connected in the triple- and fourfold-coincidence circuits has made it possible to "center" the incident particle flux with respect to the energy-measuring system.

Two versions of trigger selection of particles by their charge were used during the experiment. When the first version was used, virtually every charged particle incident on the equipment was recorded; the second version involved suppression of the contribution due to protons and α particles.

TESTING THE CHARGE-MEASURING SYSTEM

The use of four silicon detector layers offers a chance to employ various algorithms of particle charge reconstruction.

When processing the data from the charge measuring system, it was necessary that, first and foremost, the overlapping regions of the sensitive and coarse gain ranges of each detector be matched. This was achieved by using a set of calibration signals, which were simultaneously detected by two channels of an amplifier. In this case, corrections were applied for the pedestals (i.e., for the systematic shift of the amplitude) and for the difference in the gains of the electronic system: $h(n) = k_h(n)(J_h(n) + P_h(n))$ and $L(n) = k_L(n)(J_L(n) + P_L(n))$, where n is the layer number; J_h and J_L, h and L are the charge signals prior to and after applying the corrections, respectively; k_h and k_L are the corrections for the gain; and P_h and P_L are the corrections for the pedestal for the sensitive and coarse channels, respectively. The correction factors obtained during primary calibration are presented in Table 1.

It should be noted that reconstruction of charge distributions requires that both channels of each detector be calibrated with high accuracy. It is convenient to analyze data in terms of $\sqrt{h}$, and $\sqrt{L}$. In this case, the charge dependence is almost linear and small deviations from a linear law can be attributed to the nonlinear response of the equipment or the inaccurate determination of the pedestal.

The position of the peak due to single-charged particles was determined from the database for a rigidity of 157.65 GeV/Z (nearly pure protons). For multiply charged particles, peaks in the distributions on the above scales were sought for a rigidity of 339.56 GeV/Z, taking into account the possible presence of additional peaks due to simultaneous incidence of a few particles. The peak position for lithium nuclei was determined by interpolation, because excess α particles made it difficult to find the maximum in the distribution. The calibration curves obtained for the sensitive and coarse channels are shown in Figs. 3 and 4, respectively.

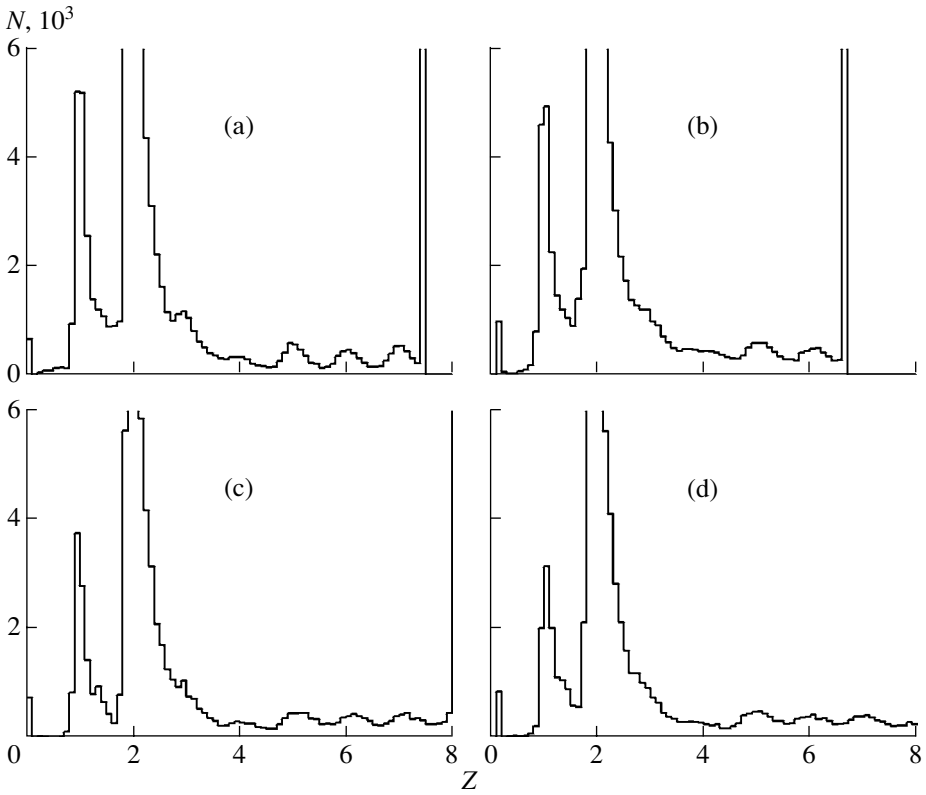

Fig. 5. Charge distributions of fragments at a rigidity of 339 GeV/*Z* for the sensitive channel: (a) the first, (b) second, (c) third, and (d) fourth layers.

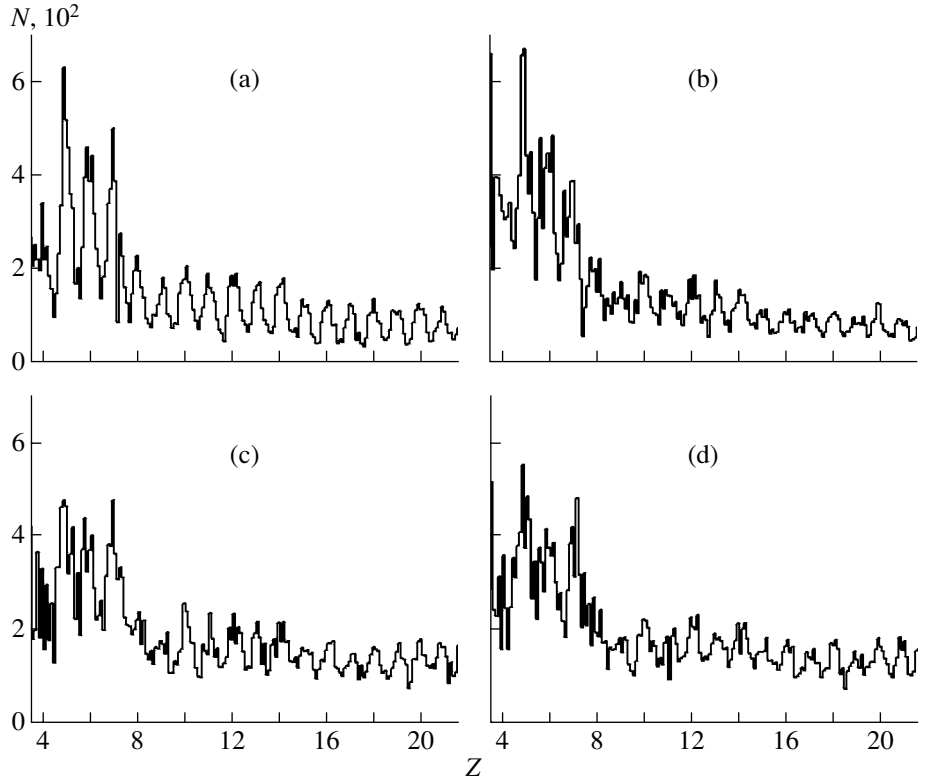

Fig. 6. Charge distributions of fragments at a rigidity of 339 GeV/*Z* for the coarse channel: (a) the first, (b) second, (c) third, and (d) fourth layers.

Table 1. Primary calibration parameters of the charge detector

n	Sensitive channel		Coarse channel	
	k_h	P_h	k_L	P_L
1	0.745	1730	1.0	1703
2	0.616	1723	1.27	1677
3	0.867	1702	0.85	1687
4	1.0	1695	0.92	1692

The calibration curves are approximated by squared relationships $Z = C_0 + C_1\sqrt{h} + C_2h$ for the sensitive channel and $Z = C_0 + C_1\sqrt{L} + C_2L$ for the coarse channel. The numerical values of the approximation parameters are presented in Table 2.

The charge distributions obtained using the above approximations are shown in Figs. 5 (for the sensitive channel) and 6 (for the coarse channel). Comparing the charge distributions of different detectors (from the first to the fourth), one can see that the first and second (downstream of the beam) detectors provide the highest accuracy and that the accuracy of the fourth detector is the worst.

The charge spectra of the four detectors were matched using the rank statistics method. For each recorded event (due to an incident particle), four charges measured by the four detectors were arranged in ascending order (regardless the detector to which a particular charge corresponded). The next step was to determine the charge that is second in magnitude, and this value was used as the estimate for the charge. It should be noted that the rank statistics method provides better results than mere averaging of values, since fluctuations of the ionization losses have a sharply asymmetrical form, as opposed to the standard distribution of errors.

Apart from the fluctuations of ionization losses, the described technique has allowed the effect of concomitant particles to be suppressed to a considerable degree. Nuclear fragmentation may produce several fragments with equal values of the A/Z ratio and, hence, with equal rigidities. This effect may be particularly important for selection of particles with a rigidity of 315.5 GV/Z, when a few α particles, deuterons, ^{6}Li atoms, and others can be produced. For the third and fourth layers of the charge detector, the probability that several particles

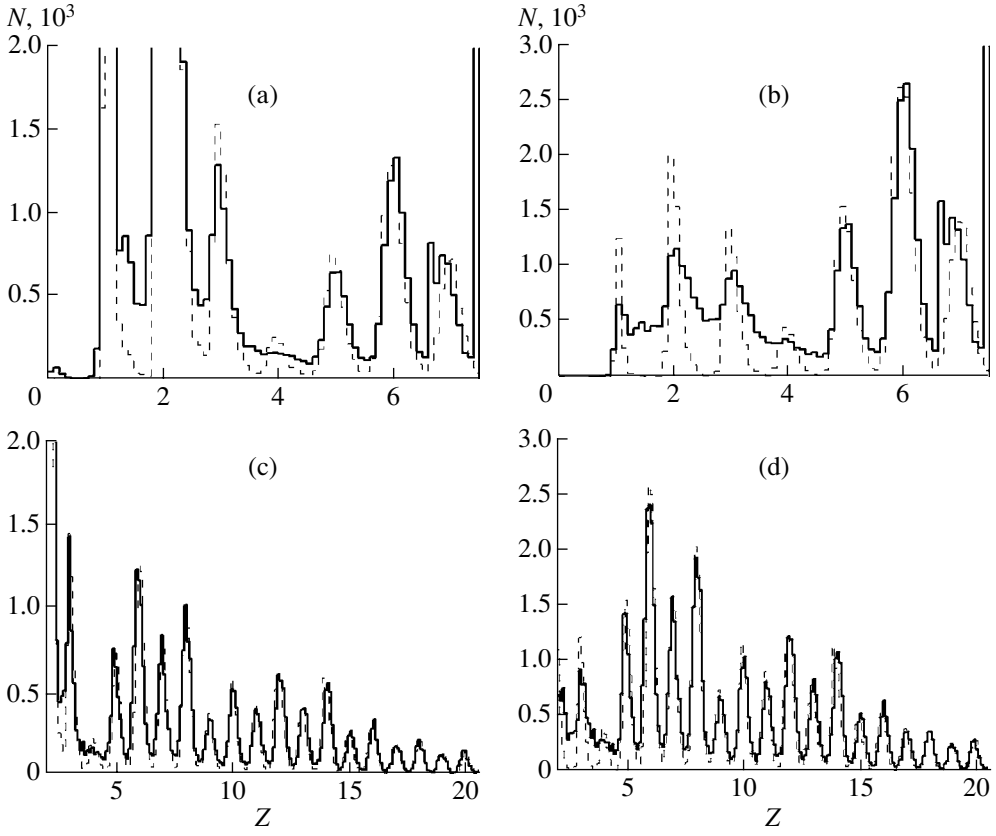

Fig. 7. Charge distributions of fragments with due account of the rank statistics at a rigidity of 315 GV/Z for (a, b) the sensitive channel and (c, d) the coarse channel at (a, c) low and (b, d) high thresholds. The experimental data are shown with a solid line, and the results of simulations using the GEANT software are presented with a dashed line.

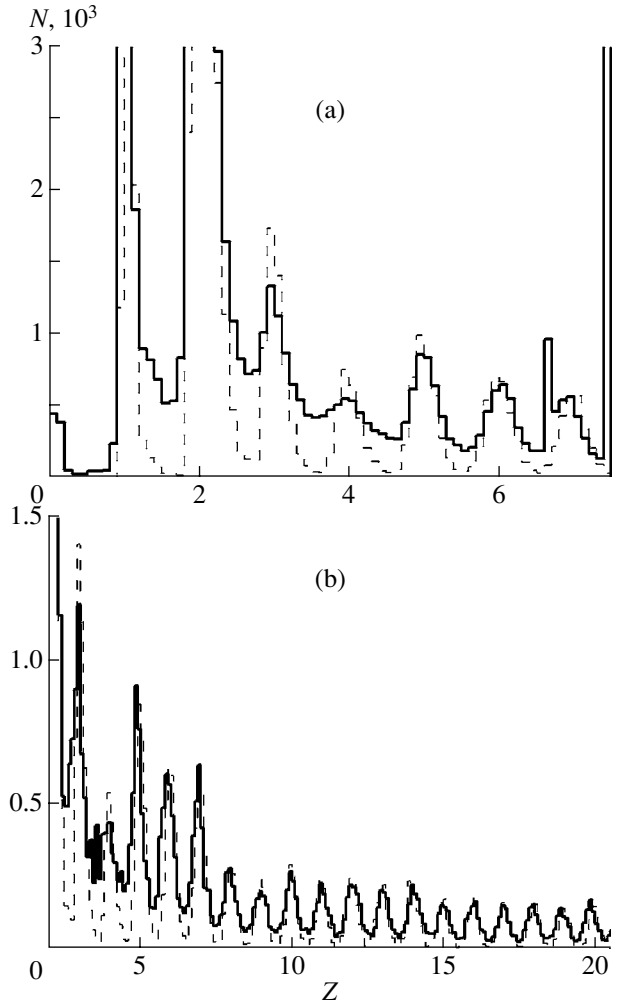

Fig. 8. Charge distributions of fragments in view of the rank statistics for (a) the sensitive channel and (b) the coarse channel at a rigidity of 339 GeV/Z and a low threshold. The experimental data are shown with a solid line, and the results of simulations using the GEANT software are presented with a dashed line.

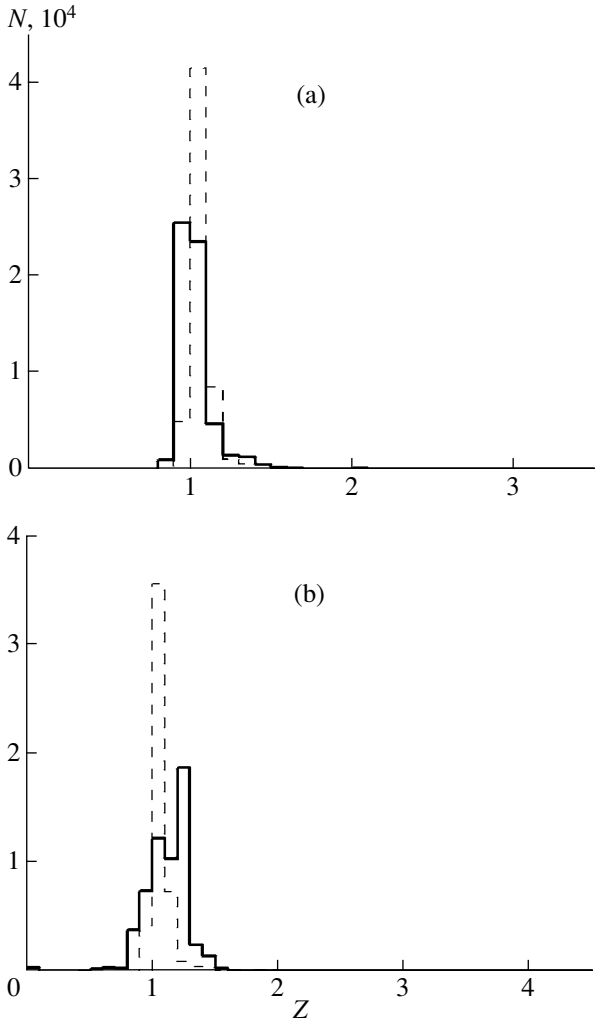

Fig. 9. Charge distributions of fragments in view of the rank statistics for (a) the sensitive channel and (b) the coarse channel at a rigidity of 158 GeV/Z and a low threshold. The experimental data are shown with a solid line, and the results of simulations using the GEANT software are presented with a dashed line.

will simultaneously hit the detector is considerably higher, owing to the larger area. However, these layers are cut off using the above technique. The average error in determining the charge is ~0.2.

As noted above, the simulation was performed using the GEANT 3.21 software package with the aim of analyzing the response of the charge-measuring system in view of the reverse current from the tungsten converter.

Table 2. Accurate calibration parameters of the charge detector

n	Sensitive channel			Coarse channel		
	C_0	C_1	C_2	C_0	C_1	C_2
1	0.084	0.1399	−0.000019	0.081	0.5632	−0.000806
2	0.100	0.1378	−0.000020	0.003	0.5748	−0.001080
3	0.039	0.1466	−0.000113	−0.036	0.5708	−0.000947
4	0.132	0.1389	−0.000020	−0.155	0.5800	−0.001130

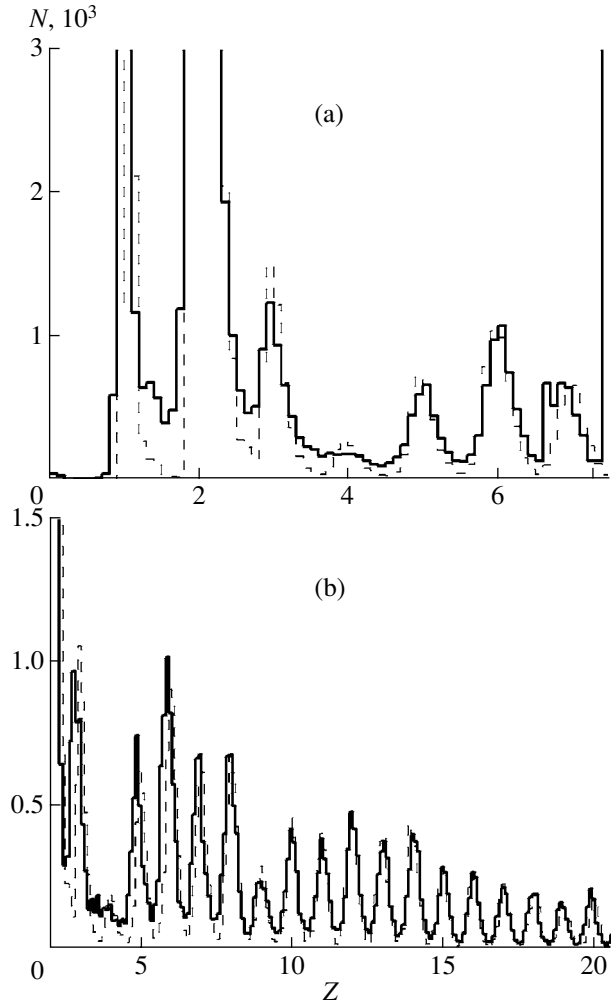

Fig. 10. Charge distributions of fragments in view of the rank statistics for (a) the sensitive channel and (b) the coarse channel at a rigidity of 319 GeV/Z and a low threshold. The experimental data are shown with a solid line, and the results of simulations using the GEANT software are presented with a dashed line.

The fraction of the component with charge Z_i was found from the experimental data as a quantity proportional to the number of events with a charge determined using the above technique in the range $[Z_i - 0.25; Z_i + 0.25]$. We simulated the structure of the prototype of the experimental setup, including the charge-measuring system, the tungsten converter, and the microstrip detector. For each layer of the charge-measuring detector, energy deposition ΔE was recorded. The analytical procedure was similar to the procedure used in the analysis of experimental data, and the charge dependence was approximated by function $Z = C_0 + C_1\sqrt{\Delta E} + C_2 E$. The parameters of approximation based on the simulation results are presented in Table 3.

Table 3. Calibration parameters of the charge detector, obtained by simulation

n	C_0	C_1, MeV$^{-0.5}$	C_2, MeV^{-1}
1	0.132	2.640	0.00088
2	0.195	2.527	0.00405
3	0.186	2.532	–0.00299
4	0.208	2.478	0.00471

Data were analyzed following the algorithm based on the rank statistics method. The charge distributions obtained experimentally and by simulation for different rigidities are shown in Figs. 7–10. They are seen to be in good agreement. A discrepancy is observed only in the region of Li–Be charges; it can be explained by the presence of concomitant particles produced during fragmentation of primary indium nuclei and incompletely cut off by the selection criteria.

Comparison of the simulation results to the experimental data confirms the validity of the above assumptions.

CONCLUSIONS

The procedure for measuring the charges of various nuclei using four arrays of pad silicon detectors has made it possible to determine the particle charges. Comparison of the charge distributions obtained in the test experiment on the accelerator to the results of simulation has demonstrated good agreement. A slight discrepancy in the range of Li–Be charges can be explained by the presence of concomitant particles produced during fragmentation of primary indium nuclei and incompletely cut off by the selection criteria.

These results lead to the conclusion that the technique for measuring the charge in the NUCLEON experiment, together with the equipment intended for this experiment, will offer a chance to measure the charge composition of high-energy CRs with an accuracy of 0.2–0.3, which is sufficient both for discriminating separate CR components and for studying the abundance of secondary nuclei in CRs at high energies.

ACKNOWLEDGMENTS

This work was supported by the Russian Foundation for Basic Research, grant nos. 05-02-16781-a and 05-02-16783-a.

REFERENCES

1. Swordy, S.P., L'Heureux, J., Meyer, P., and Muller, D., *Astrophys. J.*, 1993, vol. 403, p. 658.
2. Adams, J., Bashindzhagyan, G.L., Bashindzhagyan, P.G., et al., *Izv. Akad. Nauk, Ser. Fiz.*, 2001, vol. 65, no. 3, p. 430.
3. Zatsepin, V.I., Adams, J.H., Ahn, H.S., et al., *Nucl. Instrum. Methods Phys. Res., Sect. A*, 2004, vol. 524, p. 195.

4. Korotkova, N.A., Podorozhnyi, D.M., Postnikov, E.B., et al., *Yad. Fiz.*, 2002, vol. 65, no. 5, p. 884 [*Phys. At. Nucl.* (Engl. Transl.), vol. 65, no. 5, p. 852].
5. *GEANT User's Guide. CERN DD/EE/83/1*, Geneva, 1983.
6. Kalmykov, N.N. and Ostapchenko, S.S., *Preprint of Institute of Nuclear Physics, Moscow State University*, Moscow, 1998, no. 98-36/537.
7. Kalmykov, N.N., Ostapchenko, S.S., and Pavlov, A.I., *Nucl. Phys. B (Proc. Suppl.)*, 1997, vol. 52, p. 17.
8. Podorozhnyi, D., Atkin, E., Boreiko, V., et al., Abstracts of Papers, *Proc. 29 ICRC*, Pune, India, 2005, vol. 3, p. 361.
9. Turundaevskiy, A., Grebenyuk, V., Karmanov, D., et al., Abstracts of Papers, *Proc. 29 ICRC*, Pune, India, 2005, vol. 3, p. 365.
10. Bashindzhagyan, G.L., Voronin, A.G., Golubkov, S.A., et al., *Prib. Tekh. Eksp.*, 2005, no. 1, p. 46 [*Instrum. Exp. Tech.* (Engl. Transl.), no. 1, p. 32].